Chapter 6

Microstructural characterization and hydrothermal ageing resistance of RHA-derived amorphous and crystalline silica-doped Alumina toughened Zirconia biocomposite.

6.1 Introduction

Zirconia (ZrO_2) is a versatile bioceramic widely used in medical implants due to its exceptional mechanical strength, hardness, and wear resistance. Common applications include dental crowns, bridges, and implants in orthopedic and dental prosthetics [1]. The crystallographic phases of zirconia under atmospheric pressure- monoclinic (m), tetragonal (t), and cubic (c)-are crucial. The tetragonal-to-monoclinic (t-m) transformation at around 1000°C results in volume expansion and shear strains, impacting its use as a structural material [2]. Yttria (Y2O3) addition stabilizes the t phase, enabling stress-induced phase transformation, enhancing toughness[3]. Y-TZP (yttria-stabilized tetragonal zirconia polycrystal) is widely used, especially in hip prostheses. However, surface exposure to water can lead to hydrothermal ageing or Low Temperature Degradation (LTD), causing roughening and microcracking[4]. Studies reveal a slow t-m transformation in humid conditions, initiating microcracking and strength loss. This phenomenon contributed to a notable failure in 2001 [5].

Several Strategies have been attempted to prevent LTD, including exploring alternative ceramic materials, such as alumina–zirconia and zirconia–alumina composites, and reducing grain size or increasing yttria content in the starting powder, etc. [6][7]. However, these approaches result in reduced zirconia toughness, diminishing its mechanical appeal. Another strategy involves the addition of dopants, such as alumina, silica, copper oxide, cerium oxide, iron oxide, etc., which have proven effective in slowing down Low-Temperature Degradation (LTD) [8]. Alumina toughened zirconia (ATZ) is a preferred choice in contemporary orthopedic surgery due to its similar mechanical properties and reduced sensitivity to aging [9]. Schneider (2008) observed that an ATZ-ceramic composite (80 wt% Y-TZP and 20 wt% alumina) demonstrated decelerated aging in a humid atmosphere at body temperature over 50 years [10]. Li et al. (1997) suggested

that Al2O3 suppresses water-induced phase transformation by interacting with H_2O, forming a protective hydroxylation layer on Al2O3-dispersed particles [11]. This shields the sample surface from further interaction with H_2O and prevents LTD transformation. Accumulation of alumina in the first 5–10 monolayers significantly stabilizes zirconia and improves LTD resistance. Vleugels found the highest toughness contribution at an alumina fraction of 2.5 vol%, while a further increase (> 10 vol%) leads to alumina toughened zirconia, a material with exceptional strength [12]. As alumina addition also enhances wear resistance, ATZ becomes an intriguing material for biomedical implants. Kern et al. (2012) attempted to improve the mechanical properties of Y-TZP/alumina composites by substituting coprecipitated 3Y-TZP with tougher and more transformable 2.5Y-TZP produced through powder coating [13].

Silica emerges as a compelling dopant for enhancing the stability of 3Y-TZP. The exploration of silica's impact on the hydrothermal aging of YSZ samples dates back to 1986 when Lange et al. investigated its effects on YSZ samples, revealing that the aging phenomenon stems from water vapor, with intergranular silicate glassy phases playing an insignificant role [14]. In 1987, Mecartney studied the influence of an amorphous second phase on Y-TZP properties using silica. It was observed that samples with a higher glass phase content experienced lesser degradation, refuting the notion of stress corrosion cracking as the primary cause of degradation [15]. This study supports the idea that glass aids in reducing residual stresses from thermal expansion anisotropy. A decade later, Tan and co-workers demonstrated that the use of silica encourages the formation of intergranular glassy layers, fortifying the anti-degradation resistance of Y-TZP [16]. In 2000, Gremillard et al. illustrated the effects of small silica additions on the microstructures and mechanical properties of 3Y-TZP ceramics [17]. Silica was identified at triple junctions, resulting in a rounded microstructure and reduced internal stresses, thereby

significantly enhancing Low-temperature degradation (LTD) resistance without impacting slow crack growth (SCG) behavior [18]. Further insights from Takigawa et al. in 2009 highlighted that 0.1 mol% SiO_2 doping retards the t-m phase transformation of 3Y-TZP [19]. The presence of silicon ions segregating along grain boundaries alters the grain boundary diffusivity of hydroxyl ions, influencing phase transformation behavior. Nakamura et al. in 2011 demonstrated that silica doping led to ceramics with reduced monoclinic content, enhanced resistance to degradation, and minimal strength reduction compared to conventional Y-TZP [20,21]. In 2015, Samodurova et al. conducted a comprehensive study on silica doping, both with and without alumina co-doping in 3Y-TZP [22]. The findings indicated that silica concentration at multiple grain junctions contributed to the rounding of zirconia grains without affecting fracture mode. Co-doping with alumina and silica showcased distinct mechanisms decelerating LTD in 3Y-TZP, and their combined use increased resistance to aging without compromising material fracture toughness. Recent research by Alves et al. and Ramos et al. has further emphasized the protective role of a silica glass layer in preventing LTD and antagonistic wear [23,24]. Additionally, this layer enhances bondability to resin cement when applied to the inner surface. Collectively, these studies underscore the efficacy of silica, whether used as a dopant or as an outer layer material in Zirconia-based ceramics, as an exceptional means of reducing LTD. Notably, while various forms of silica exist, including crystalline and amorphous, there remains a gap in understanding the optimal form for mitigating LTD in Zirconia-based bioceramics.

In addition to traditional methods utilizing additives and dopants for enhancing the resistance to Low-Temperature Degradation (LTD) and other properties of bioceramics, there is a growing interest in exploring alternative solutions that not only tackle these challenges but also bring about economic advantages while reducing waste [25]. The

circular economy, especially within the bioeconomy framework, has emerged as a promising strategy endorsed by global experts to address the intricate and interconnected issues in this domain [26]. In recent decades, silica derived from Rice Husk (RH), an agricultural byproduct, has garnered attention as a cost-effective source of silica [27]. Both amorphous and crystalline forms of silica can be derived from RH under suitable conditions [28]. Given that millions of tons of rice are produced globally annually, resulting in approximately 200 kg of RH generated per metric ton of rice [29], the proper disposal of RH presents a considerable challenge due to its expansive surface area and carbon content, which can contribute to environmental pollution. Researchers have endeavored to utilize RH effectively, either by directly reinforcing it with other components or utilizing it as ash to harness its high silica content [30]. Rice husk consists of major constituents such as hydrated silicon, cellulose, and lignin [31]. Various methods, encompassing chemical and thermal treatments, have been employed to synthesize silica from RH, with thermal treatment being the preferred method [32,33]. The silica produced from RH necessitates minimal grinding owing to the highly reactive nature of the silica particles, representing a noteworthy advantage of this process.

The present research aims to identify the optimal form of silica (amorphous/crystalline) to be used as an additive in ATZ biocomposites for improved LTD resistance. Additionally, the research aims to advance the principles of biocircularity in biomaterial production by incorporating waste-derived silica from Rice Husk. A comparative study has been conducted on both amorphous and crystalline silica derived from Rice Husk Ash (RHA), considering hydro-aging, mechanical performance, and other characterizations as key parameters. This research not only seeks to enhance the performance of bioceramics but also aligns with sustainable practices by repurposing agricultural waste in biomaterial production.

6.2 Materials and Methodology

The principal constituents employed in the production of silica-doped ATZ biocomposites are zirconia, alumina, and rice husk ash (RHA). Zirconia powder, characterized by an average grain size of 20 nm, was procured from Merck, Germany. High-purity alumina powder, sourced from ALCOA ACC, CT 3000SG in Mumbai, Maharashtra, India, was utilized in this investigation. ATZ powder was synthesized by blending alumina and zirconia in a weight ratio of Alumina: Zirconia: 4:1, followed by 24 hours of pot milling. Silica for the study was derived from residual RHA waste obtained from agricultural harvesting, with rice husk collected from a local farm. The harvested rice husk underwent washing with both normal tap water and deionized (DI) water to ensure the complete removal of dust particles and soil content. The washed rice husk was subsequently oven-dried at 110°C until completely dry. The resulting rice husk powder underwent thermal treatment, yielding two types of silica: amorphous (below 800°C) and crystalline silica (above 1000°C). The powder was then milled using a rotary mill equipped with iron blades and sieved to obtain particles smaller than 150 μm using appropriate sieves. The fabrication of samples involved the dry pressing method with sucrose solution as a binder, resulting in rectangular samples measuring 40 by 10 by 10, prepared using a Hydraulic press with a 10-ton load. Thermal treatment was conducted at temperatures of 1400°C and 1500°C. The sucrose (Merck, India) and DI used were of analytical grades.

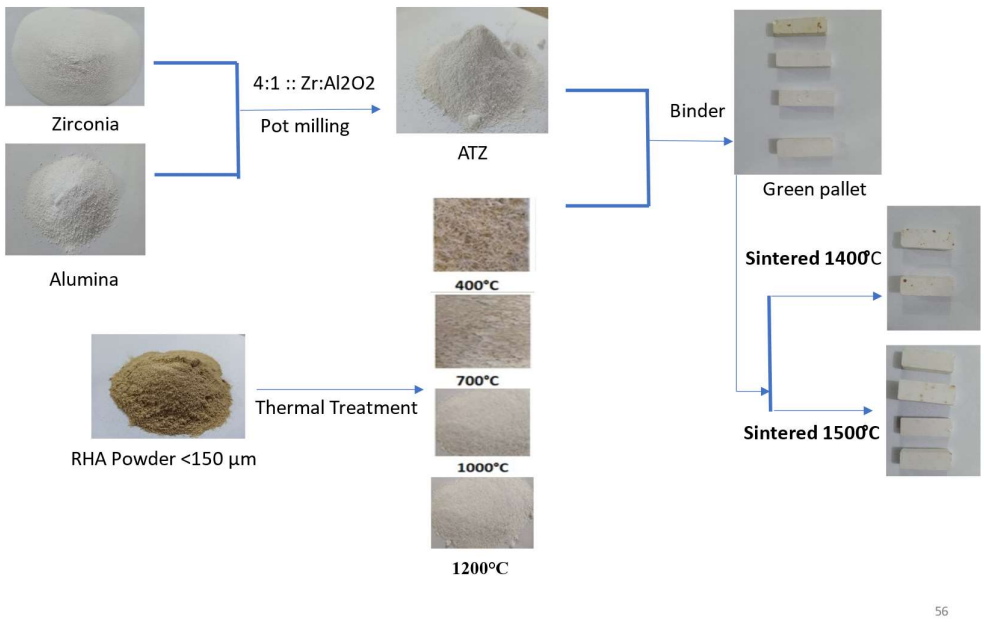

Figure 6.1. Preparation of silica-doped Alumina Toughened Zirconia (ATZ) biocomposites are zirconia, alumina, and Rice Husk Ash (RHA)

The apparent porosity of the sintered silica-ATZ biocomposite was determined by employing the water immersion technique based on Archimedes' principle. X-ray diffraction (XRD) analysis was performed to analyze the diverse phases within the samples. The surface morphology of the silica-doped ATZ biocomposite was investigated using Scanning Electron Microscopy (SEM) with an FEI Inspect S30 (Sweden) instrument. Hydrothermal aging (HA) was conducted in an autoclave following the protocol established by the International Organization for Standardization (ISO 13356): 134 ◦C, 2 bar pressure (ISO 13356, 2015), for a duration of 24 hours. The bioactivity assessment of doped and undoped samples involved immersion in a modified simulated body fluid (1.5×SBF). The 1.5×SBF, with ion concentrations 1.5 times higher than standard simulated body fluid (SBF) per Kokubo and Takadama's recommendation, had its pH adjusted to 7.4 using HCl

and Tris-hydroxymethyl-aminomethane. Each sample underwent immersion in 40 ml of 1.5×SBF, maintained at a constant temperature of 36.5°C for one week. Bioactivity was evaluated through SEM analysis, focusing on observing a characteristic apatite-like layer.

6.3 Results and Discussion

6.3.1- Microstructural Evolution

The comprehensive analysis of the ATZ composite material reveals a dual influence of silica addition on grain growth within the structure. Initially, the amalgamation of both amorphous and crystalline silica derived from Rice Husk (RH) instigates observable grain growth in the composite's zirconia and alumina components, indicating a significant influence on the microstructure. This resultant grain growth facilitates the filling of intercrystalline gaps, leading to improved densification (Fig. 1). However, a critical threshold is identified, as grain growth is impeded beyond 5 wt% silica addition. Remarkably, this inhibitory effect is accompanied by the conversion of excess silica into a glassy phase, effectively incorporating alumina and zirconia grains into this phase. The less frequently encountered glassy silica phase, typically found at the triple junction of grains when silica is below 5 wt%, is homogeneously distributed along the grains of zirconia and alumina after exceeding 5 wt% amorphous silica content. The predominantly polygon-shaped grains in pure ATZ samples become rounder due to amorphous silica addition, achieving nearly spherical shapes when silica doping surpasses 5 wt%.

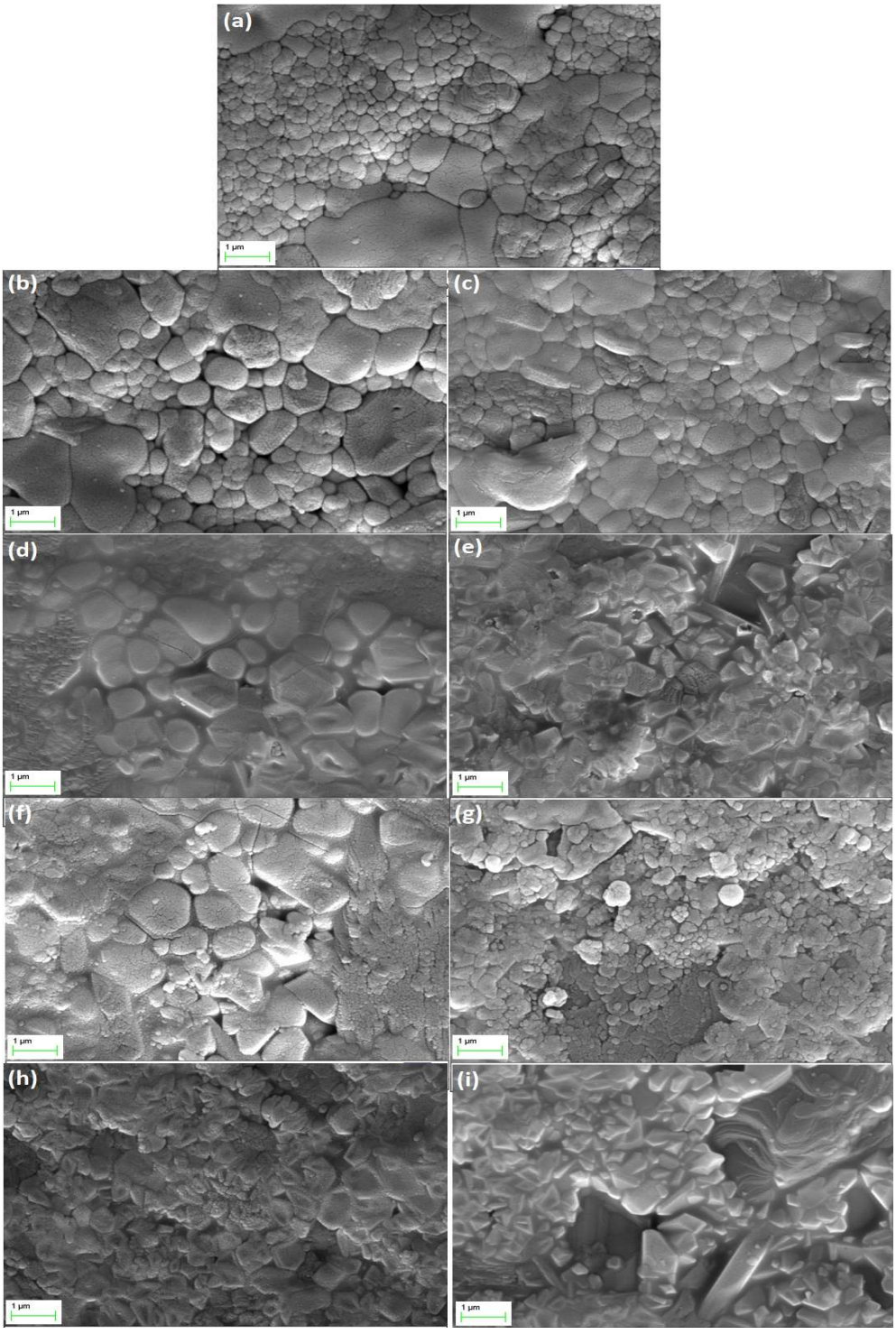

Figure 6.2. Scanning Electron Microscope (SEM) micrograph showing

(a)- Pure Alumina Toughened Zirconia (ATZ),

(b)- 1% wt amorphous silica doped ATZ,

(c)- 5% wt amorphous silica doped ATZ,

(d)- 10% wt amorphous silica doped ATZ,

(e)- 15% wt amorphous silica doped ATZ,

(f)- 1% wt crystalline silica doped ATZ,

(g)- 5% wt crystalline silica doped ATZ,

(h)- 10% wt crystalline silica doped ATZ,

(i)- 15% wt crystalline silica doped ATZ.

However, these rounded grains transform into either acicular or sharply edged polygons when excess silica is incorporated, as evidenced by the figures when silica content reaches 15 wt%. The differentiation between amorphous and crystalline silica becomes evident, with amorphous silica demonstrating superior grain growth and densification compared to its crystalline counterpart. However, the dispersion of alumina and zirconia grains and their reduced growth achieved with higher amorphous silica doping (beyond 5 wt%) is observed for crystalline silica at lower content (below 5 wt%). This disparity could be attributed to the more effective conversion of crystalline silica to the glassy phase compared to amorphous silica within that specific temperature range. Consequently, it is observed that the more rounded shapes of alumina and zirconia grains are prevalent in amorphous silica-doped ATZ samples across a wider range of doping levels compared to crystalline silica. Another notable observation in ATZ samples with higher silica doping is the appearance of line crack fractures on the surface of the glassy phase. These cracks, considered flaws, may be attributed to mismatched cooling behaviors resulting from the thermal expansion properties of the glassy phase in contrast to those of alumina and zirconia grains.

6.3.2 Effect of Rice Husk Ash (RHA) silica on Bulk Density of Alumina Toughened Zirconia (ATZ) composite:

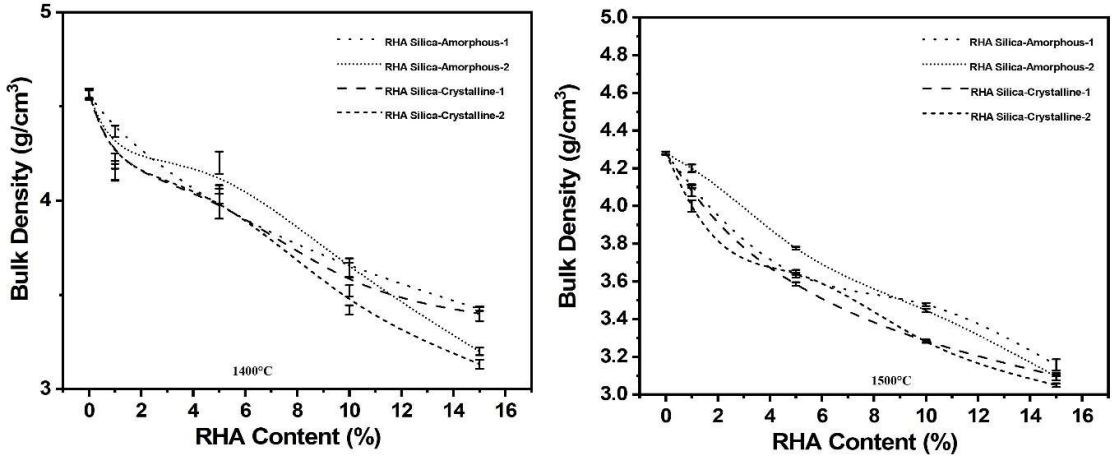

Figure 6.3. Bulk density variation of silica-doped Alumina Toughened Zirconia (ATZ) samples concerning Rice Husk Ash (RHA) content.

The bulk density (BD) characteristics of the Silica-doped Alumina Toughened Zirconia (ATZ) composite exhibit a nuanced relationship with the type and percentage of Rice Husk Ash (RHA) silica, as well as the sintering temperature (Fig. 6.3). Notably, an increase in amorphous RHA silica content corresponds to a decrease in bulk density, a trend similarly observed with crystalline RHA silica. This observation suggests that both types of silica contribute to a reduction in bulk density as their content increases. Moreover, a direct comparison between amorphous and crystalline silica reveals that amorphous silica consistently yields better bulk density, emphasizing its positive impact on densification within the composite, as also evident from the SEM micrographs. The bulk density of Silica-doped ATZ varies within the range of 4.3% to 3.1%, illustrating the sensitivity of bulk density to different percentages of silica. Interestingly, the densification performance is further influenced by the sintering temperature, with higher temperatures at 1500°C proving more effective than 1400°C, as evidenced by the maximum bulk density reaching 5.39 at 1500°C compared to 4.36 at 1400°C.

6.3.3 Effect of Rice Husk Ash (RHA) silica on Porosity of Alumina Toughened Zirconia (ATZ) composite

The apparent porosity (AP) characteristics of Silica-doped Alumina Toughened Zirconia (ATZ) provide valuable insights into the impact of silica type, percentage, and sintering temperature on the material's porosity (Fig. 6.4). Notably, amorphous silica is found to result in lower apparent porosity compared to crystalline silica as also suggested by bulk density data. The apparent porosity of Silica-doped ATZ exhibits variation within the range of 4.3% to 3.1% for different percentages of silica at 1400°C and remains under examination for 1500°C. When comparing amorphous and crystalline silica, the former consistently yields lower AP, as illustrated in the figures where the maximum AP is recorded as 4.36 for amorphous silica and 4.16 for crystalline silica.

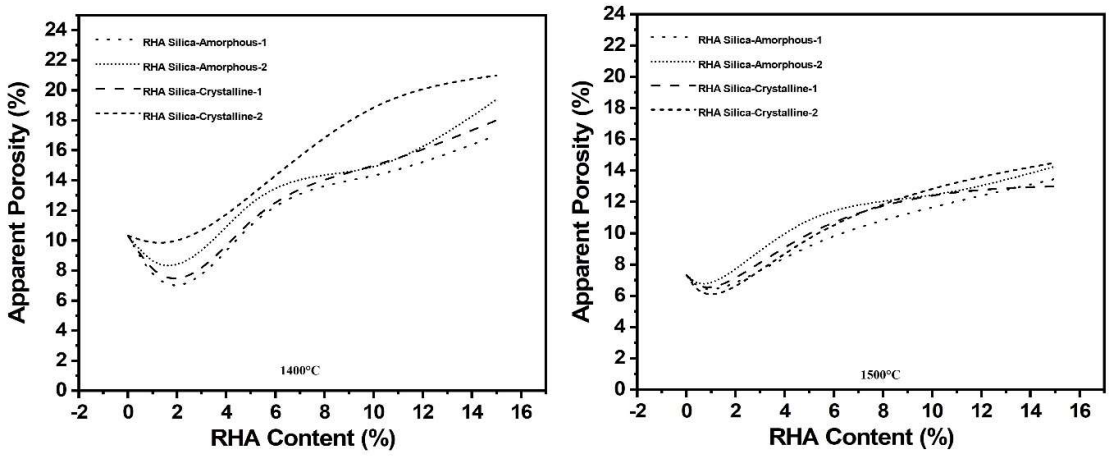

Figure. 6.4. Apparent porosity variation of silica doped Alumina toughened zirconia (ATZ) samples to Rice husk ash (RHA) content.

A noteworthy observation is the inverse relationship between bulk density (BD) and apparent porosity, as an increase in silica content leads to a decrease in bulk density for both amorphous and crystalline silica. Furthermore, the sintering temperature significantly influences bulk density, with 1500°C exhibiting superior densification compared to 1400°C, resulting in maximum bulk densities of 4.36 and 5.39, respectively.

6.3.4 Effect of Rice Husk Ash (RHA) silica on Bending strength of Alumina Toughened Zirconia ATZ composite:

Bending results consistently correlate with Bulk Density and Apparent Porosity metrics, complemented by robust support from Microstructural characterization. The bending strength of silica-doped Alumina Toughened Zirconia (ATZ) biocomposite displays a marginal enhancement of up to 1% silica doping (Fig. 6.5). This effect is observed for both amorphous and crystalline silica variants. The observed increase in strength is attributed to the improved compaction and grain growth of alumina and zirconia grains facilitated by the presence of silica. The glassy phase of silica contributes to enhanced grain growth and densification. However, the escalating silica doping concentration beyond 1 wt% results in a decline in strength. This decline is attributed to an increased presence of the glassy phase, ultimately leading to reduced bulk density and strength of the ATZ material. A comparative analysis of amorphous and crystalline silica reveals that amorphous silica-doped samples exhibit slightly superior strength compared to their crystalline counterparts. This difference is explained by the enhanced compaction facilitated by amorphous silica, as discussed in the preceding section.

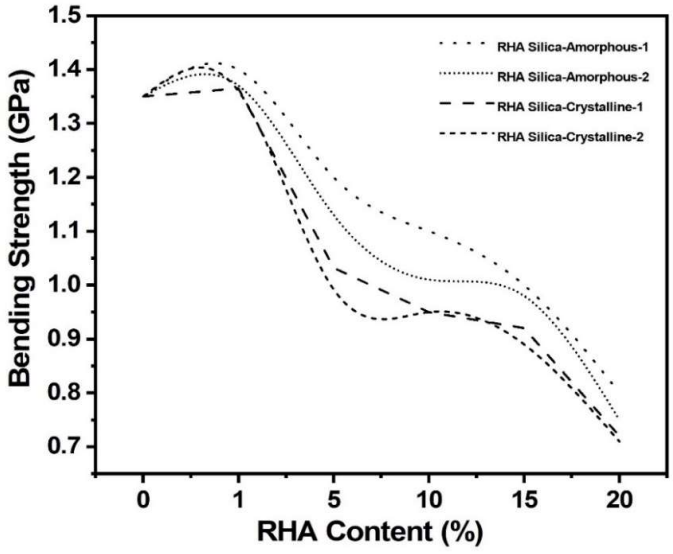

Figure. 6.5. Bending strength variation of silica-doped Alumina toughened zirconia (ATZ) samples concerning Rice husk ash (RHA) content.

6.3.5 X-Ray Diffraction Analysis

The X-ray diffraction (XRD) analysis of the composite material reveals a distinctive alteration in the crystalline phases, notably in the zirconia component, consequent to the introduction of silica (Figure. 6.6). A significant outcome is the observed transformation of the triclinic phase of zirconia to the monoclinic phase, indicating a structural modification induced by the presence of silica. Amorphous silica, in particular, demonstrates a heightened efficiency in facilitating the conversion of triclinic zirconia to the monoclinic phase when compared to its crystalline counterpart.

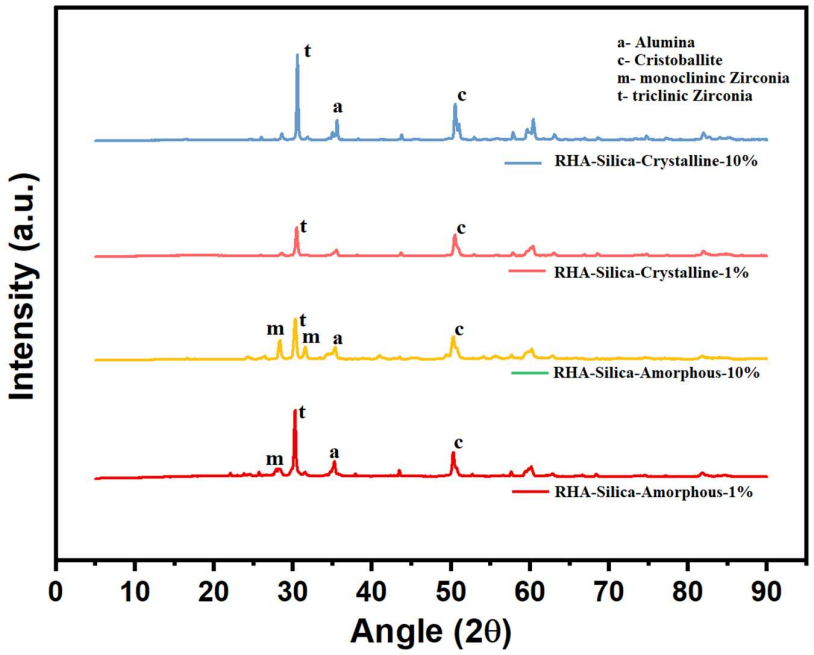

Figure. 6.6. X-ray diffraction pattern of silica-doped alumina-toughened zirconia (ATZ) composites.

6.3.6- Hydrothermal Aging Characterization

The inherent challenges associated with zirconia (YSZ) biocomposites include their susceptibility to hydrothermal aging or low-temperature degradation (LTD), necessitating advancements in YSZ samples through specific doping. While ATZ demonstrates improved resistance to hydrothermal aging, there is still room for enhancement. Silica

emerges as a promising dopant to augment the hydrothermal aging resistance of zirconia-based biocomposites, aligning with prior research findings that attribute silica's role in forming a glassy protective layer and inducing grain rounding, thereby reducing stress concentration.

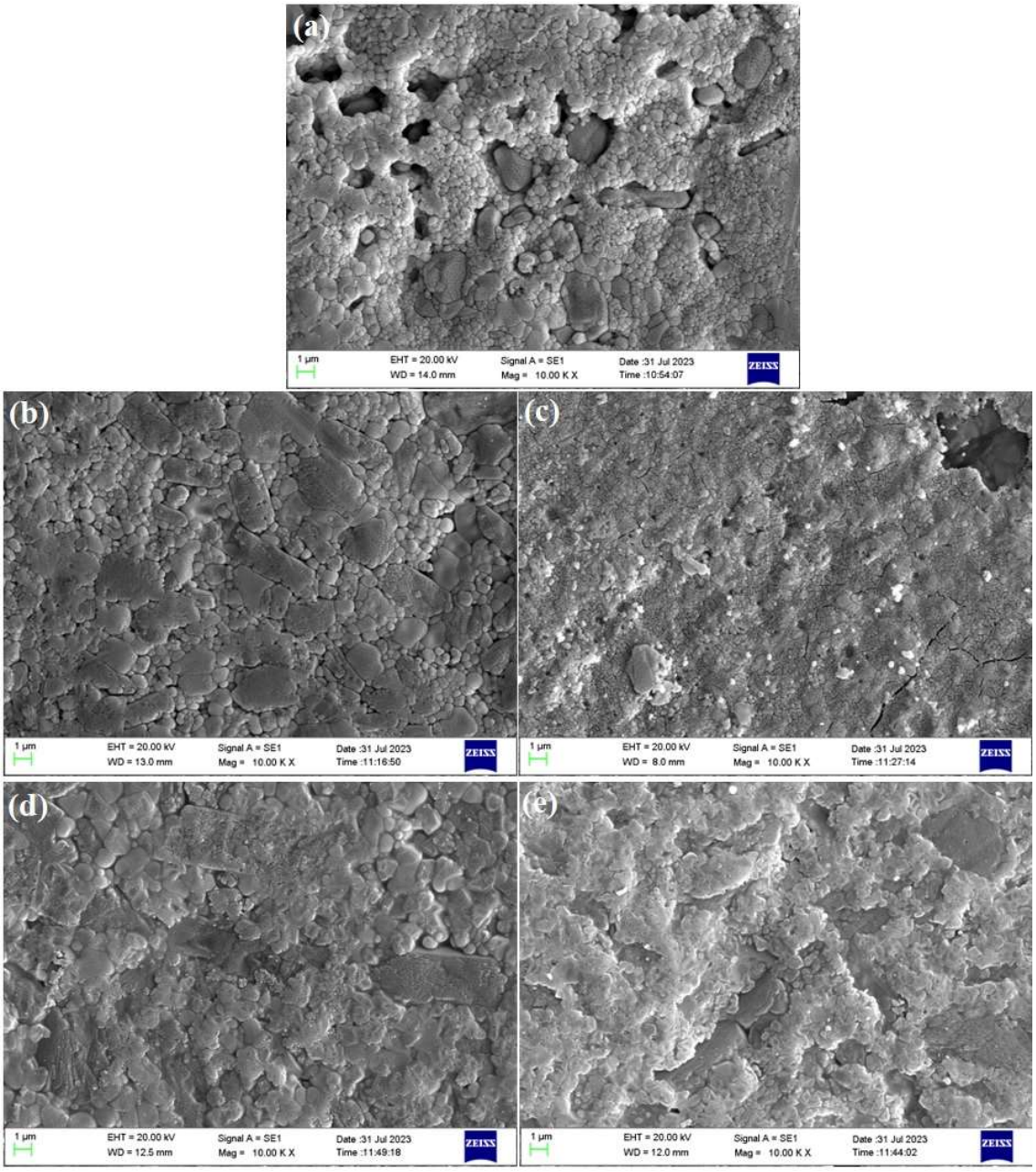

Figure. 6.7. Scanning Electron Microscopy (SEM) micrograph after hydrothermal aging of

(a)- Pure Alumina Toughened Zirconia (ATZ),

(b)- 1% wt amorphous silica doped ATZ,

(c)- 10% wt amorphous silica doped ATZ,

(d)- 1% wt crystalline silica doped ATZ,

(e)- 10% wt crystalline silica doped ATZ.

Our study corroborates these findings, revealing enhanced LTD resistance with silica doping, as evidenced by SEM microstructures (Fig. 6.7) of doped and undoped ATZ samples. Unmistakably, undoped ATZ samples, after 24 hours of hydrothermal aging, exhibit loosening of alumina grains from zirconia grains, indicating vulnerability to fracture toughness under hydrothermal conditions. In contrast, SEM images of silica-doped ATZ samples clearly depict intact alumina and zirconia grains, preserving the material's strength even after hydrothermal aging. A comparative analysis of amorphous and crystalline silica doping in ATZ and their impact on hydrothermal aging highlights the superior LTD resistance of amorphous silica over crystalline silica. This disparity may be attributed to the enhanced densification and grain growth achieved through amorphous silica or the reduced glassy phase provided by amorphous silica compared to crystalline silica at similar doping percentages. Nevertheless, optimal results for both amorphous and crystalline silica doping are obtained around 1 wt%, indicating that higher silica content compromises LTD resistance. Higher silica content introduces more glassy phase, leading to hairline fractures on the surface due to hydrothermal aging, as observed in SEM micrographs, and increased loosening of alumina and zirconia grains in ATZ. Conclusively, our observations suggest that a lower percentage of amorphous silica doping (1 wt%) represents the most favorable strategy for enhancing the LTD resistance of ATZ-based biocomposites.

6.3.7 Biological Characterizations

Biological characterization was conducted through in vitro bioactivity tests to evaluate the ability of amorphous silica-doped Alumina Toughened Zirconia (ATZ) samples to stimulate apatite formation, and the results were compared with those of pure ATZ samples.

The composites were immersed in a simulated body fluid (SBF) solution for one week. Significant morphological changes were observed on the scaffold surfaces following immersion in SBF. Within the initial week, apatite layers formed on both undoped and doped ATZ samples, with each scaffold surface displaying a distinct white apatite deposition (Fig. 6.8). After seven days of immersion, the pure ATZ composite exhibited minimal apatite crystal growth on its surface. In contrast, the incorporation of silica into ATZ led to densely populated apatite crystal deposition, indicating an augmentation in nucleation and growth rates of apatite facilitated by silica addition. SEM images further illustrated that amorphous silica-doped ATZ samples derived from Rice Husk Ash (RHA) exhibited superior bioactivity compared to pure ATZ, aligning with higher material bioactivity as depicted in Figure 9. These findings suggest that the addition of silica not only enhances resistance to low-temperature degradation (LTD) but also improves the bioactivity of the ATZ composite.

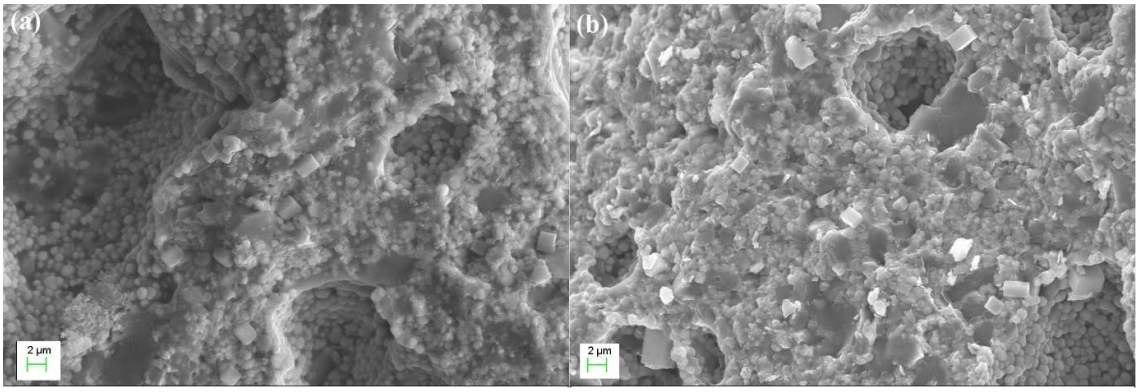

Figure. 6.8. Scanning Electron Microscope (SEM) micrograph after Simulated Body Fluid (SBF) test (a)- Pure ATZ, (b)- 1% wt amorphous silica doped ATZ

6.4 Conclusions

In conclusion,

1. The comprehensive investigation into the impact of silica doping on the properties of the developed ATZ biocomposite has provided valuable insights into the intricate relationships among microstructure, physico-mechanical attributes, and biological behavior.

2. Rice Husk Ash (RHA) as a silica source has been established as a reliable means to enhance the material's characteristics. The study highlights that doping silica up to 5 wt% in ATZ contributes to increased grain growth of zirconia particles; however, higher wt% of silica leads to reduced grain growth in both alumina and zirconia particles, adversely affecting the mechanical properties of the biocomposite. Notably,

3. The comparison between amorphous and crystalline silica reveals that amorphous silica demonstrates superior grain growth and densification of ATZ samples.

4. The significance of the silica doping level is evident, with physical and mechanical properties experiencing enhancement up to 1 wt% doping. Beyond this threshold, a notable and significant decrease in these properties is observed.

5. Hydrothermal aging resistance is improved with silica doping, particularly amorphous silica, showing superior resistance to crystalline silica. The optimal results for aging resistance are obtained with up to 1 wt% silica doping, beyond which a decline is noted.

6. Furthermore, the positive influence of silica doping on bioactivity is underscored by the increased hydroxyapatite layer.

7. The research demonstrates that RHA is a suitable source for obtaining silica, which can be effectively utilized as an additive, particularly in the amorphous form derived from RHA, to enhance the mechanical and aging properties of ATZ biocomposites.

8. These findings contribute to the ongoing exploration of advanced biomaterials, offering promising avenues for developing improved biocompatible materials with enhanced performance in biomedical applications.

References

[1] N.M. Alfrisany, G.M. De Souza, Surface and bulk properties of zirconia as a function of composition and aging, J. Mech. Behav. Biomed. Mater. 126 (2022) 104994. https://doi.org/10.1016/j.jmbbm.2021.104994.

[2] A. Kocjan, J. Cotič, T. Kosmač, P. Jevnikar, In vivo aging of zirconia dental ceramics – Part I: Biomedical grade 3Y-TZP, Dent. Mater. 37 (2021) 443–453. https://doi.org/10.1016/j.dental.2020.11.023.

[3] M.K.G. Abbas, S. Ramesh, K.Y. Sara Lee, Y.H. Wong, C.Y. Tan, U. Johnson Alengaram, P. Ganesan, F. Musharavati, E. Zalnezhad, Densification of copper oxide doped alumina toughened zirconia by conventional sintering, Ceram. Int. 48 (2022) 6287–6293. https://doi.org/10.1016/j.ceramint.2021.11.171.

[4] L. Gremillard, C. Wei, J. Chevalier, K. Hans, T. Oberbach, A fast, stepwise procedure to assess time-temperature equivalence for hydrothermal ageing of zirconia-based materials, J. Eur. Ceram. Soc. 38 (2018) 181–186. https://doi.org/10.1016/j.jeurceramsoc.2017.08.018.

[5] J. Chevalier, L. Gremillard, S. Deville, Low-temperature degradation of zirconia and implications for biomedical implants, Annu. Rev. Mater. Res. 37 (2007) 1–32. https://doi.org/10.1146/annurev.matsci.37.052506.084250.

[6] Q. Jing, F. Zhang, L. Lei, J. Zhang, Improving low temperature degradation of 3Y-TZP ceramics via high temperature carburizing, Ceram. Int. 49 (2023) 11865–11874. https://doi.org/10.1016/j.ceramint.2022.12.033.

[7] Y. Tufan, J. Park, A. Öztürk, B. Ercan, Enhanced bioactivity and low temperature degradation resistance of yttria stabilized zirconia/clay composites for dental applications, J. Eur. Ceram. Soc. 42 (2022) 7300–7310. https://doi.org/10.1016/j.jeurceramsoc.2022.08.039.

[8] S. Ramesh, K.Y. Sara Lee, C.Y. Tan, A review on the hydrothermal ageing behaviour of Y-TZP ceramics, Ceram. Int. 44 (2018) 20620–20634. https://doi.org/10.1016/j.ceramint.2018.08.216.

[9] H. Tsubakino, K. Sonoda, R. Nozato, Martensite transformation behavior during isothermal aging in partially stabilized zirconia with and without alumina addition, J. Mater. Sci. Lett. 12 (1993) 196–198. https://doi.org/10.1007/BF00819957.

[10] J. Schneider, S. Begand, R. Kriegel, C. Kaps, W. Glien, T. Oberbach, Low-temperature aging behavior of alumina-toughened zirconia, J. Am. Ceram. Soc. 91 (2008) 3613–3618. https://doi.org/10.1111/j.1551-2916.2008.02700.x.

[11] J.F. Li, R. Watanabe, Influence of a small amount of Al2O3 addition on the transformation of Y2O3-partially stabilized ZrO2 during annealing, J. Mater. Sci. 32 (1997) 1149–1153. https://doi.org/10.1023/A:1018567414745.

[12] J. Vleugels, Z.X. Yuan, O. Van Der Biest, Mechanical properties of Y2O3/Al2O3-coated Y-TZP ceramics, J. Eur. Ceram. Soc. 22 (2002) 873–881. https://doi.org/10.1016/S0955-2219(01)00389-2.

[13] F. Kern, R. Gadow, Alumina toughened zirconia from yttria coated powders, J. Eur. Ceram. Soc. 32 (2012) 3911–3918. https://doi.org/10.1016/j.jeurceramsoc.2012.03.014.

[14] F.F. Lange, G.L. Dunlop, B.I. Davis, Degradation During Aging of Transformation-Toughened Materials at 250 ° C, 40 (1986) 237–240.

[15] Y.T.Z.P. Y, M.L. Mecartney, Influence of an Amorphous Second Phase on the Properties of, 58 (1987) 54–58.

[16] H.C. Tan, C. Gill, S. Lawson, The Effect of Sintering Additives on the Hydrothermal and Corrosive Degradation of Y-TZP, Key Eng. Mater. 113 (1995) 199–206. https://doi.org/10.4028/www.scientific.net/KEM.113.199.

[17] L. Gremillard, T. Epicier, J. Chevalier, G. Fantozzi, MICROSTRUCTURAL STUDY OF SILICA-DOPED ZIRCONIA CERAMICS, 48 (2000) 4647–4652.

[18] L. Gremillard, J. Chevalier, T. Epicier, G. Fantozzi, Improving the Durability of a Biomedical-Grade Zirconia Ceramic by the Addition of Silica, 407 (2002) 5–7.

[19] Y. Takigawa, T. Shibano, Y. Kanzawa, K. Higashi, Effect of Small Amount of Insoluble Dopant on Tetragonal to Monoclinic Phase Transformation in Tetragonal Zirconia Polycrystal, 50 (2009) 1091–1095. https://doi.org/10.2320/matertrans.MC200832.

[20] T. Nakamura, H. Usami, H. Ohnishi, M. Takeuchi, H. Nishida, T. Sekino, The effect of adding silica to zirconia to counteract zirconia ' s tendency to degrade at low temperatures, 30 (2011) 330–335. https://doi.org/10.4012/dmj.2010-142.

[21] T. Nakamura, H. Usami, H. Ohnishi, H. Nishida, X. Tang, The relationship between

milling a new silica-doped zirconia and its resistance to low-temperature degradation (LTD): a pilot study, 31 (2012) 106–112. https://doi.org/10.4012/dmj.2011-048.

[22] M. V Swain, A. Samodurova, Acta Biomaterialia The combined effect of alumina and silica co-doping on the ageing resistance of 3Y-TZP bioceramics, (2014). https://doi.org/10.1016/j.actbio.2014.09.009.

[23] L. Marcia, M. Alves, S. Rodrigues, N. De Carvalho, J. Buizastrow, T. Moreira, B. Campos, M. Antonio, Y. Zhang, Silica infiltration on translucent zirconia restorations : Effects on the antagonist wear and survivability, Dent. Mater. 38 (2022) 2084–2095. https://doi.org/10.1016/j.dental.2022.11.015.

[24] N.C. Ramos, L.M.M. Alves, P. Ricco, G.M.A.S. Santos, M.A. Bottino, T.M.B. Campos, R.M. Melo, Strength and bondability of a dental Y-TZP after silica sol-gel infiltrations, Ceram. Int. 46 (2020) 17018–17024. https://doi.org/10.1016/j.ceramint.2020.03.288.

[25] J.K. Wang, Ç. Çimenoğlu, N.M.J. Cheam, X. Hu, C.Y. Tay, Sustainable aquaculture side-streams derived hybrid biocomposite for bone tissue engineering, Mater. Sci. Eng. C. 126 (2021). https://doi.org/10.1016/j.msec.2021.112104.

[26] E. Santolini, M. Bovo, A. Barbaresi, D. Torreggiani, P. Tassinari, Turning agricultural wastes into biomaterials: Assessing the sustainability of scenarios of circular valorization of corn cob in a life-cycle perspective, Appl. Sci. 11 (2021). https://doi.org/10.3390/app11146281.

[27] E. Elimbinzi, S.S. Nyandoro, E.B. Mubofu, J.C. Manayil, A.F. Lee, K. Wilson, Valorization of rice husk silica waste: Organo-amine functionalized castor oil templated mesoporous silicas for biofuels synthesis, Microporous Mesoporous Mater. 294 (2020). https://doi.org/10.1016/j.micromeso.2019.109868.

[28] N.S. Zainal, Z. Mohamad, M.S. Mustapa, N.A. Badarulzaman, A.Z. Zulkifli, The ability of crystalline and amorphous silica from rice husk ash to perform quality hardness for ceramic water filtration membrane, Int. J. Integr. Eng. 11 (2019) 229–235. https://doi.org/10.30880/ijie.2019.11.05.029.

[29] K. Mohanta, D. Kumar, O. Parkash, Properties and Industrial Applications of Rice husk : A review, Int. J. Emerg. Technol. Adv. Eng. 2 (2012) 86–90.

[30] A. Pattnayak, N. Madhu, A.S. Panda, M.K. Sahoo, K. Mohanta, A Comparative study on mechanical properties of Al-SiO2 composites fabricated using rice husk silica in crystalline and amorphous form as reinforcement, Mater. Today Proc. 5 (2018) 8184–8192. https://doi.org/10.1016/j.matpr.2017.11.507.

[31] T.G. Korotkova, S.J. Ksandopulo, A.P. Donenko, S.A. Bushumov, A.S. Danilchenko, Physical properties and chemical composition of the rice husk and dust, Orient. J. Chem. 32 (2016) 3213–3219. https://doi.org/10.13005/ojc/320644.

[32] R.A. Bakar, R. Yahya, S.N. Gan, Production of High Purity Amorphous Silica from Rice Husk, Procedia Chem. 19 (2016) 189–195. https://doi.org/10.1016/j.proche.2016.03.092.

[33] A. Gupta, V. Pandey, M.K. Yadav, K. Mohanta, M.R. Majhi, A comparative study on physico-mechanical properties of silica compacts fabricated using rice husk ash derived amorphous and crystalline silica, Ceram. Int. 48 (2022) 35750–35758. https://doi.org/10.1016/j.ceramint.2022.07.098.